The solution of tetrabutylammoniumiodide in formamide: investigation of the surface by MIES

1991 J. Phys.: Condens. Matter 3 5639

(http://iopscience.iop.org/0953-8984/3/29/016)

J. Phys.: Condens. Matter 3 (1991) 5639–5655. Printed in the UK

The solution of tetrabutylammoniumiodide in formamide: investigation of the surface by MIES

H Morgner, J Oberbrodhage, K Richter and K Roth

Naturwissenschaftliche Fakultät, Universität Witton/Herdecke, D-5 810 Witten-Annen, Federal Republic of Germany

Received 11 February 1991, in final form 3 May 1991

Abstract. We have studied the surface of the solution of tetrabutylammoniumiodide (TBAI) in formamide (FA). The extreme surface sensitivity of metastable impact electron spectroscopy allows us to state that the anions I^- are part of the topmost layer. This was not unambiguously predictable from previous experiments and not borne out by standard model concepts. The model that we propose on the basis of our own and published data characterizes the surface at high concentrations as dominated by two-dimensional TBAI clusters. These clusters begin to form at molalities around 0.1 and are sensitive to temperature before they stabilize at higher molal concentrations.

1. Introduction

Due to its small observation depth of a few Ångströms electron spectroscopy is an ideal tool for studying the effect of surface segregation in binary liquid mixtures [1] and in solutions [2–5]. UPS has been demonstrated to make visible the fact that different salts show very different surface activity depending on their chemical nature. Solutions of the inorganic salt NaI in several solvents showed no trace of the salt in UPS [2]. In view of the observation depth of an estimated 10 Å in UPS this result signals that the solvation shell separates both Na^+ and I^- ions from the surface by at least this distance. The situation is distinctly different for a salt like tetrabutylammoniumiodide (TBAI) whose hydrophobic butyl groups give strong surface activity in any polar solvent. Indeed, TBAI is clearly made visible by UPS [2].

A more detailed study of the surface segregation of TBAI salts was performed by means of ESCA by the group led by H Siegbahn [3–5].

For a 0.5 molal solution of TBAI in formamide (FA) they found the surface concentration of the salt enhanced by a factor of three compared with the bulk concentration and a segregation depth of 15 Å [3]. This result was achieved by varying the angle of observation of the emitted electrons with respect to the liquid surface. Assuming a fixed electron mean free path this varies the effective observation depth. In a later study they found that the length of the alkyl groups in the tetra-alkylammonium salt positively influences the effect of segregation. The elemental and chemical sensitivity of ESCA allows the segregation of cations and anions to be studied separately. No differential behaviour was found for I^- or ClO_4^- with respect to the cations, whereas NO_3^- ions appear to be less abundant in the surface layer than their counter ions.

0953-8984/91/295639+17$03.50

The interpretation of these data has been attempted [5] by employing the double-layer model developed in electrochemistry for the interface between electrolyte and a metal electrode [6]: those ions that adsorb specifically at the electrode form the first Helmholtz plane attracting counter ions which constitute a second plane (Gouy plane). It depends on the particular electrolyte considered whether the counter ions have solvation shells as in the bulk, thus forming a diffuse second layer or are attached more closely to the ions in the first Helmholtz plane, either separated by a shared solvent molecule or even in direct contact. These concepts have been used [5] to discuss the situation of the free surface of the electrolyte. The property of specific adsorption at the electrode is replaced at the liquid/vacuum interface by the tendency of the hydrophobic alkyl groups to drive the cation to the surface. As mentioned earlier, a strong segregation of the cations at the surface is indeed observed [3–5]. The question then in terms of the double-layer model is whether the negative counter ions form a diffuse second layer or are in close contact with the cations which sit at the very surface. From the results mentioned earlier [3–5] the authors concluded that this would depend on the kind of anion. With respect to the cations TBA^+ the iodine ions I^- as well as the ClO_4^- ions are in close contact whereas the NO_3^- ions appear to form a diffuse second layer. Moberg *et al* [5] found that this behaviour correlates with the activity of the respective salts as transfer catalysts.

The depth resolution of neither UPS nor angular-resolved ESCA is sufficient to discern whether contact ion pairs are oriented parallel or perpendicular to the surface. The model picture from electrochemistry described earlier would suggest a perpendicular orientation in which the anion is hidden from the outermost surface layer. However, the crystal structures of related complexes such as TBAI trihalides [7] teach us that a plane containing both TBA^+ ions and anions is clearly compatible with the electrostatic and chemical interactions between the ions.

In the present study we are able to show unambiguously that the I^- ions of the TBAI salt appear in the outermost surface layer. This is possible by making use of the perfect surface sensitivity of metastable impact electron spectroscopy (MIES). Furthermore, some information on the lateral surface structure can be derived from our data.

The paper is organized as follows: in the next section we describe a new machine, designed for MIES and UPS studies of liquid surfaces. The experimental data for a broad range of TBAI concentration in FA are given in section 3. The last section contains our interpretation of the data and the information that can be derived.

2. Experimental details

In this section we describe a new machine for electron spectrometric studies of liquid surfaces by MIES and UPS which has been designed and built over the last few years. Our previous apparatus had been a molecular beam machine [8] provisionally equipped with a liquid target [9].

The new design differs from the old one in the following respects:

(i) the pumping efficiency is improved;

(ii) sampling times are greatly reduced due to the much higher luminosity of the electron spectrometer;

(iii) as far as possible all sensible parts are removed from the target chamber in order to achieve higher reliability of operation; and

(iv) a strictly modular design of the primary (He*, photon) beam, liquid target and electron spectrometer makes servicing easier and less time-consuming.

As before [8, 9], the vacuum system is composed of four separate chambers all equipped with turbomolecular pumps. Two of the chambers serve to produce the primary beam. One houses the cold discharge for the production of metastable helium atoms and HeI photons, the corresponding pumping speed being 510 l s^{-1}. The second chamber (330 l s^{-1}) contains the facilities for beam purification: a quenching lamp for removal of the He(2^1S) component from the beam if desired and a condenser that allows the removal of ions and the field ionization of atoms in Rydberg states. The dispersive parts of the electron spectrometer, including the channel-plate detector, are in the third chamber with a pumping speed of 170 l s^{-1}. The liquid target is in the fourth chamber which is equipped with a turbomolecular pump which works at 330 l s^{-1} and a liquid nitrogen cryopump with an active area of 490 cm^2. Assuming a sticking coefficient of unity the calculated pumping speed for the solvent under study, FA, is 3300 l s^{-1}. A valve of inner diameter 25 cm separates the cryopump from the vacuum vessel. This allows the loaded pump to be exchanged with a new one without exposing the rest of the machine to air.

The working pressure in the target chamber amounts typically to $2\text{–}3 \times 10^{-3}$ Pa, in the electron spectrometer chamber the value is usually below 10^{-4} Pa.

As before [9] we separate the effects of the metastable helium atoms and the HeI photons by a time-of-flight technique. For this purpose we use a commercial light beam chopper. It is housed in the same chamber as the quenching lamp. After removing the side covers of the chopper we obtain stable operation of the instrument in the vacuum without cooling. The chopping cycle of 266 μs on the basis of 62.5 rev s^{-1} is achieved by a chopper wheel with 60 slits. Adjustment of the gate width to the cycle length (1:4) is made possible by mounting a second chopper wheel with the proper phase shift adjacent to the first one. The distance between the axis of the chopper and the centre of the beam is 47.5 mm. This results in a slit width of 1.24 mm. Since the thickness of the chopper wheels is not small compared with our effective slit the sense of rotation has to be properly chosen as shown in figure 1.

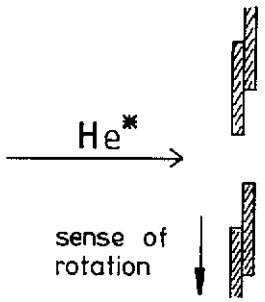

Figure 1. Cross section of the chopper wheel in the plane of the high voltage, He*-beam. Components of a commercial light beam chopper are used. The chopper wheel consists of two disks that are turned against each other to yield the proper ratio of gate width to cycle time (0.25). A new adjustment of this ratio to values between 0 and 0.5 is easily possible.

The liquid surface is realized as a vertical liquid beam as in [9]. The liquid to be investigated is in contact with stainless steel, Pyrex glass and Teflon. From a reservoir

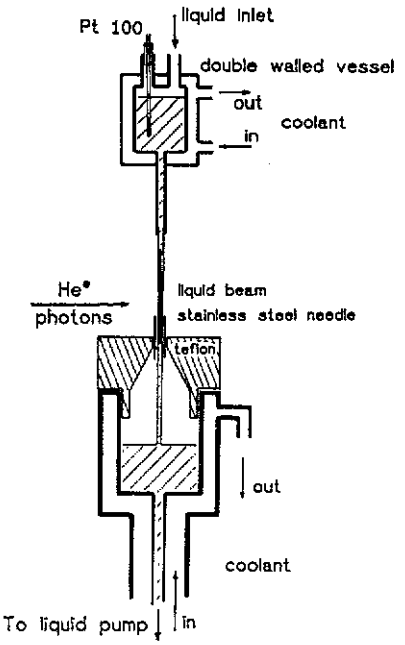

Figure 2. Central part of the liquid target.

the liquid is pushed by its own gravity to a centrifugal pump which causes less vapour bubble production than the previously used geared pump.

The liquid is guided by stainless steel and Teflon tubes to the reaction centre about 120 cm above the pump (figure 2). It passes a vessel that serves as a buffer to retain the final vapour bubbles and to give them time to recondense. From the buffer the liquid flows vertically downwards by a few centimetres to the stainless steel outlet above the reaction zone where the beam of He* and HeI-photons hits the liquid surface. To ensure electrostatic stability we have added a stainless steel needle in the centre of the liquid beam which is in galvanic contact with the outlet. With this modification the electron spectrum shifts exactly as expected under the influence of the voltage U_{ext} of up to 400 V applied between the outlet and the entrance slit of the spectrometer for suppressing gas phase contributions in the spectrum. Our working condition is $U_{ext} = 200$ V.

The temperature of the liquid is kept as constant as possible over the whole circuit. This is achieved by double-wall tubing wherever possible containing a liquid that is pumped to and from a temperature bath. Its temperature can be set between -40 and $+150\,^{\circ}C$.

In between runs we are able to remove all or part of the investigated liquid without breaking vacuum. This is achieved by a valve at the lowest point of the circuit to which an evacuated vessel can be connected. Adding liquid is easier since it is pushed into the system by the air pressure. With these possibilities it is easily possible to investigate the effect of varying the composition of a binary mixture of liquids or changing the concentration of a solution as in the present study.

The cross section of the electron spectrometer is shown in figure 3. The tandem of two 127° condensers reduces the background signal compared with that from a single condenser. The linear dimensions are doubled with respect to the previous

instrument [9]. This should result in a fourfold luminosity. Furthermore, we have replaced the channeltron from [9] by a channelplate detector followed by an eightfold anode which should increase our sampling efficiency by another factor of eight.

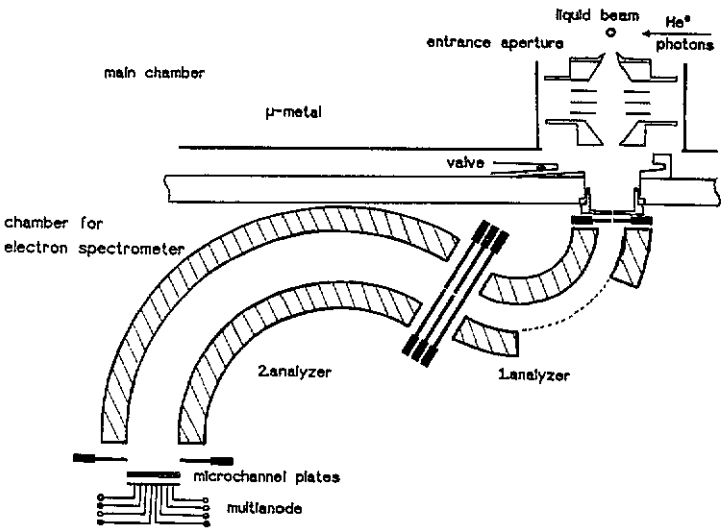

Figure 3. Cross section of the electron spectrometer.

For a given resolution E and counts per channel the necessary sampling time is reduced by a factor of 30 compared with the expected value of 32. The comparison with the previous instrument can only be approximate since the shape of the transmission functions are not the same. The structure of the spectra as taken with both instruments is the same. Thus, we conclude that the ratio of the two transmission functions is a smooth function of energy and accordingly the two transmission functions as well.

Data sampling and process control are performed by a VME-bus system which is interfaced to a computer (Atari 1040 ST) via a VME-bus interface (GTI mbH). The operation of the system is explained with the aid of the block diagram in figure 4.

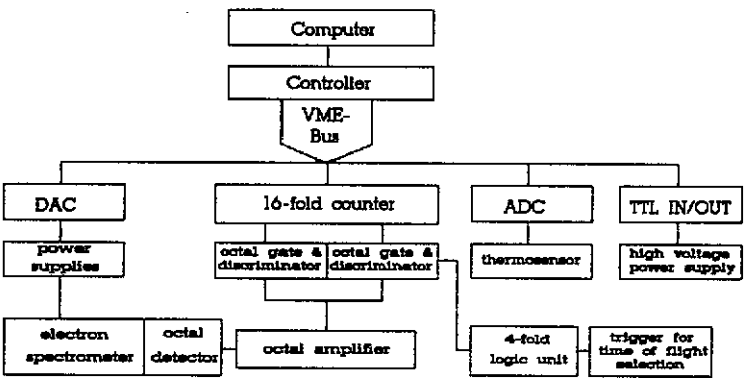

Figure 4. Block diagram of data sampling and process control. For further details see text.

The DAC unit has 8-bit exits that are used to set all voltages which are to be kept constant during the recording of an electron spectrum. One 16-bit exit serves to sweep the retarding/accelerating field preceding the 127°-condensers. A second 16-bit DAC exit allows the electron optics to be adjusted during the sweep. For a given retarding/accelerating voltage the signals from the eightfold anode are amplified (EG&G, FTA 820 A) and lead to the inputs of two eightfold gates (EG&G, CF8000).

One gate is open during recording of the MIES data, the other gate passes signals that are due to UPS, depending on the time within the time-of-flight cycle for the primary beam. The gates are controlled by a logic unit (EG&G, CO 4010) whose range of delay times has been modified to a maximum of 200 μs. The logic unit itself is synchronized by a signal derived from the chopper.

After the time set for sampling at a given retarding/accelerating voltage is over, the data from the 16-fold counter are read out and stored in the computer. After a preset number of sweeps is completed we have a total of 16 spectra, eight of them due to MIES and the rest containing UPS data. If MIES by the singlet He(2^1S) is investigated, we end up with 16 MIE spectra, eight with the quenching lamp on and eight with the quenching lamp off. In each group the eight spectra are shifted against each other due to the different positions of the eight anodes. The eight spectra of each group are added compensating for this shift.

The VME-bus is also constructed to perform such tasks as recording the machine parameters such as liquid target temperature, pressure etc via an ADC-unit. TTL outputs which can be synchronized with the sweeping time for the electron spectrum can be used to switch the quenching lamp. This option not only allows He(2^3S) to be investigated by MIES but also by the other metastable component He(2^1S).

3. Experimental results

The electron energy spectrum from the surface of a TBAI–FA solution as obtained under the impact of He(2^3S) atoms (MIES) is shown in figure 5(a). A spectrum from the surface of pure FA is displayed for comparison.

At kinetic energies larger than the FA contributions we observe structure which can be assigned to ionization of the I^- anion which is expected to carry the orbitals with the lowest ionization potential within the TBAI molecule. For the identification of the rest of the TBAI contribution it would be helpful to know the spectrum of the isolated TBAI molecule. Unfortunately, this is impossible since TBAI decomposes upon evaporation [2]. Thus, one can only try to inspect the properties of related molecules. The alkylhalides appear to be good candidates. Their orbital structure is known from UPS data and SCF calculations [10]. For the alkyliodides one finds that the binding energy of the highest occupied orbital ($5pI^-$) is smaller than that of the next orbital by a few eV. We conclude that this is also true for TBAI. This would allow the intensity of the composite TBAI–FA at a kinetic energy of 10.2 eV to be assigned overwhelmingly to FA. The scaling factor of the pure FA spectrum in figure 5(a) has been chosen with this criterion in mind. Consequently, we consider the difference between these two spectra as being solely due to TBAI, see figure 5(b). Another observation strongly supports this point of view: increase in the TBAI molal concentration leads to a monotonic decrease in absolute intensity at the position of the FA band at $E_{kin} \sim 10.2$ eV, but to an increase in intensity at the energy positions $E_{kin} \sim 12.6$ and ~ 8.4 eV.

For comparison with figure 5 we show spectra taken with HeI photons instead of He* atoms in figures 6(a) and (b). In MIES as well as in UPS we observe that

the TBAI contributions at the highest kinetic energy are composed of two peaks. As suggested by knowledge of halogen-containing molecules [10] and as done in [2] we identify the two peaks with the formation of the two fine-structure states of iodine $^2P_{1/2}$, $^2P_{3/2}$ upon ionization of I^-. As an interesting and important result we note that for the fine-structure splitting we observe values that scatter around 0.9 eV. This is surprisingly close to the splitting of the free iodine atom which is $E[^2P_{1/2}]-E[^2P_{3/2}] = 1.5 \cdot \zeta = 0.943$ eV [11]. In contrast to this the typical fine-structure splitting of halogen that forms part of molecules like halogen hydrides or the previously mentioned alkylhalides amounts to values close to ζ or two-thirds of the atomic splitting. In alkyliodides we have values between 0.55 and 0.62 eV [10] to be compared with $\zeta_{\text{Iodide}} = 0.628$ eV [11]. The fine-structure splitting observed from our MIES data is shown in figure 7 as a function of TBAI molal concentration. At the highest concentration we find the splitting essentially coincides with the atomic value. Down to a molality of approximately 0.15 this value remains constant. On the basis of the data in figure 7 we cannot exclude the possibility that the splitting decreases at very low concentrations. The splitting evaluated from a UPS spectrum taken at a molal concentration 0.34 confirms the MIES value within experimental error.

The branching ratio of the fine-structure states differs between MIES and UPS. As can be seen in table 1, MIES leads to the statistically expected value of two within experimental error whereas UPS populates both fine-structure components more or less equally. A similar behaviour is known from the ionization of Xe which is isoelectronic to I^-. MIES populates the $Xe^+(^2P_{1/2}, ^2P_{3/2})$ states essentially according to statistical expectation [12] with small deviations that are well understood [13] and remain small for He^* atoms of thermal velocities. In contrast, photoionization as a function of photon energy produces branching ratios between 1.3 and 2.2 [14, 15]. From the smaller fine-structure splitting of I compared with Xe^+ and from the fact that final state fine-structure effects should be very small in the case of $I^- \rightarrow I(^2P_{1/2}, ^2P_{3/2})+e^-$ ionization due to the neutrality of the ionized species one would expect a branching ratio that deviates from two to a lesser extent than in the case of Xe. One may conclude that the observed UPS value close to unity is due to matrix effects. No comparison with VUV-photoionization of I^- in the gas phase is possible due to lack of data.

Table 1. Experimental branching ratio in $I^-/I(^2P_{3/2})/I(^2P_{1/2})$ ionization in the surface.

Ionization process	Molal concentration	Branching ratio $I(^2P_{3/2})/I(^2P_{1/2})$
MIES	0.14	2.2 (2)
MIES	0.31	1.8 (2)
MIES	0.93	1.9 (2)
UPS	0.34	1.1 (2)

Another quantity that we can evaluate from our spectra is the area of the $I^-/I(^2P_{1/2}, ^2P_{3/2})$ peaks normalized to the area of the first band of FA. Since these peaks lie close together we expect little influence on this ratio from the unknown transmission function of our electron spectrometer. We have applied a small correction after considering the number of electrons whose ionization is represented by the peak areas being compared. In principle, any of the six 5p electrons of I^- can be

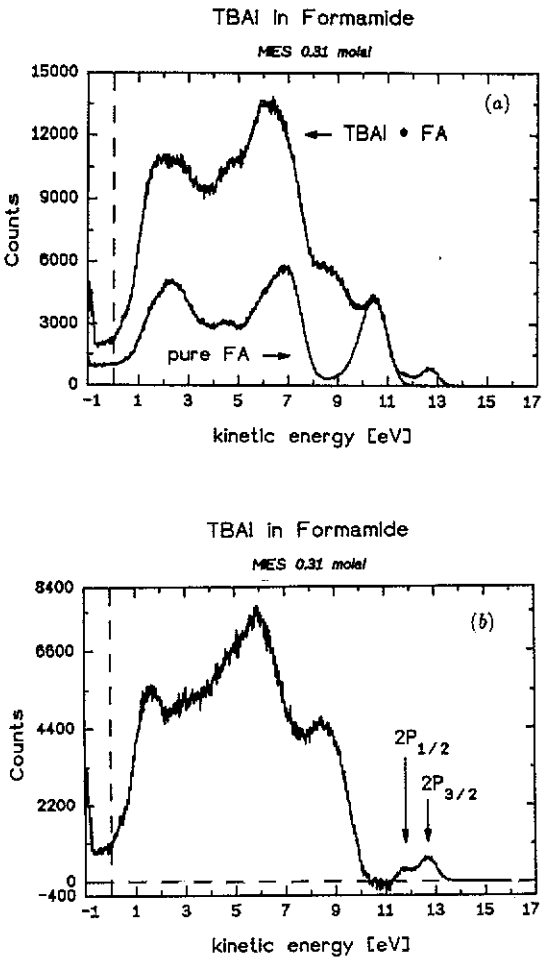

Figure 5. (*a*) Electron energy spectrum of the 0.31 molal solution of TBAI in FA, as obtained by MIES. The spectrum of pure FA is scaled so as to represent the FA contribution in the spectrum of the solution. (*b*) MIE spectrum of TBAI, obtained as difference between the two spectra in (*a*).

removed in the process $I^- \rightarrow I + e^-$. However, from He* Penning ionization in the gas phase [13, 16] it is known that MIES only probes orbitals according to their local electron density at the core of He*. This reduces the number of electrons contributing to the I^- ion to two. However, the first band of liquid FA as observed by MIES shows a minor influence from the n_0-orbital in addition to the major contribution from the $n_N(\pi_{C=O})$ orbital [9, 17]. The n_0-contribution amounts to 14(1)% of the total strength of the first band. The MIES data shown in figure 8 are corrected for this contribution. Thus, the peak areas being compared apply to the possible ionization of two electrons in both cases. Provided that the ionization cross section per electron is the same in both cases the ratio in figure 8 would directly measure the ratio of the number of I^- ions against the number of FA molecules in the outermost liquid layer. Due to lack of better information we equate the two relevant cross sections. In doing so, we obtain a good agreement with the ESCA data of H Siegbahn as discussed in section 4 of this paper.

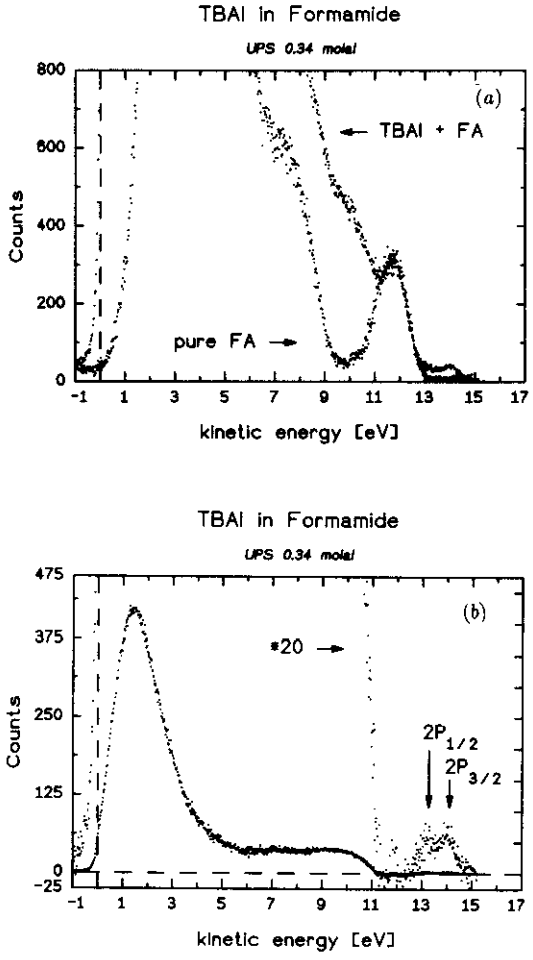

Figure 6. Same as figure 5(*a*) and (*b*), but spectra taken by UPS for molal concentration of 0.34.

Inspection of figure 8 shows that the data scatter strongly between runs, in particular in the range of molal concentrations between 0.1 and 0.25. Above $M = 0.5$ and below $M = 0.7$ the data points show a smooth behaviour. We traced this effect and found a striking correlation between the measured values and the temperature of the sample. In all cases we have a systematic ordering of the values: provided we find a temperature dependence at all the relative number of I^- ions in the outermost surface layer accessible by MIES appears to get larger with decreasing temperature. This is an interesting and apparently very strong effect which we plan to investigate more closely in the future.

Furthermore, our spectra allow the variation of peak energies to be evaluated with reference to the vacuum level as a function of molal concentration of TBAI. The values for the $I^-/I(^2P_{3/2})$ peak and the first band of FA are given in figure 9. With increasing TBAI concentration the kinetic energies of both peaks become larger, i.e. the apparent binding energies are reduced. The separation between both peaks remains constant within experimental error. This indicates that a global influence affecting solvent

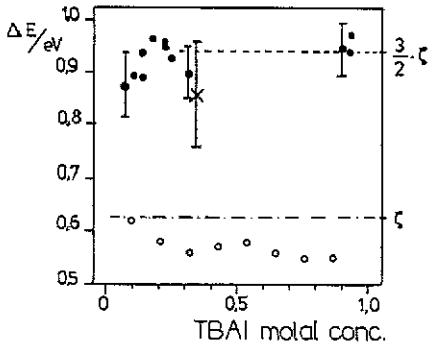

Figure 7. Fine-structure splitting observed in $I^-/I(^2P_{1/2},^2P_{3/2})$ ionization. Dots, from the surface of TBAI solution in FA as function of molal concentration, from MIES; crosses, from UPS for molality 0.34. The fine-structure splitting of the isolated iodide atom ($2/3^*\zeta$) is added as reference; circles, the fine-structure splitting as found in the gas phase by UPS for alkyliodide molecules [10] for comparison; these values have no relation to the X-axis; they are arranged from left to right with the ordering: methyl-, ethyl-, propyl-, isopropyl-, n-butyl-, isobutyl-, s-butyl, t-butyl-iodide.

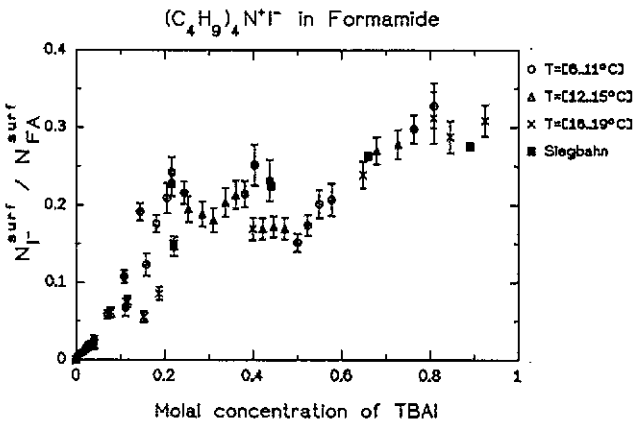

Figure 8. Number of I^- ions normalized to the number of FA molecules found by MIES as function of molality. The evaluation is based on equal detection probability for 5p electrons in I^- and n_N electrons in FA molecules. Different symbols indicate the temperature of the measurements. The number of TBA^+ ions normalized to FA molecules in the surface as derived from ESCA data by Siegbahn *et al* [4] is indicated by filled quadrangles. For further explanation see text.

and solute equally is probably responsible for this energy variation. We note that this behaviour is different from that of the binary liquid mixture of benzylalcohol and FA [1]. There, the observed different energy variations for both components were interpreted in terms of the relaxation energy which depends on the local environment of the ionized species.

For the molal concentration ($m = 0.34$) we have measured the binding energy for $I^-/I(^2P_{3/2})$ ionization from our UPS data to obtain $E_{bind}I^-/I(^2P_{3/2}) = 6.75(5)$ eV. From this value we would expect the corresponding peak in the MIES spectrum at the

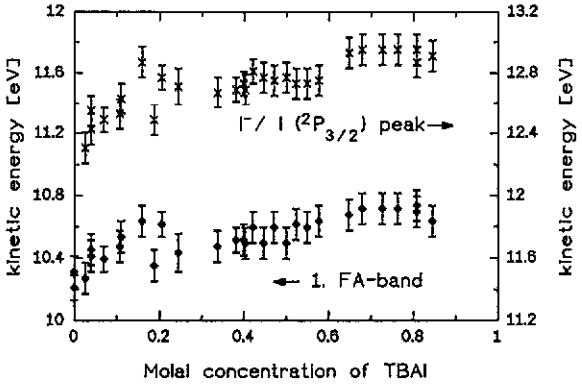

Figure 9. MIES of TBAI–FA solutions. The kinetic energies of the $I^-/I(^2P_{3/2})$ peak and of the peak maximum of the first band of FA are evaluated with respect to the zero energy edge of the spectra as function of molal concentration.

nominal value

$$E_0 = E[He^*(2^3S)] - E_{bind}[I^-/I(^2P_{3/2})] = 13.07(5)\ eV.$$

However, the kinetic energy that we find in our MIES spectrum at the same TBAI concentration is only 12.7 eV. The energy difference of 0.37(10) eV is readily understood. As known from gas phase Penning ionization of polar molecules by $He(2^3S)$ for H_2O [16], FA [18] and benzylalcohol [19] the metastable helium atoms run on an attractive potential when approaching the negative end of the molecule. This converts part of the electronic excitation energy of $He(2^3S)$ into kinetic energy which is then missing in the ionization process. Thus, we are not surprised to find the same effect when He^* gets close to the I^- embedded in the liquid surface.

4. Discussion

The key results from our data are twofold: first, I^- ions appear in the topmost layer; and second, they find themselves in a surprisingly isotropic environment.

We begin by discussing the first feature and the abundance of the I^- ions as found by MIES in the outermost layer. Provided that MIES has the same sensitivity for FA and I^- we have roughly one I^- ion in the surface per three FA molecules at a molal concentration of $m = 0.9$, see figure 8. Based on our experience with gas phase Penning ionization [16, 18] we conceive that it is possible to have a higher MIES-sensitivity for I^- than for FA but not *vice versa*. Thus, it may be possible that the relative number of I^- ions in the outermost layer is smaller than indicated in figure 8. It is interesting in this situation to compare this with the ESCA data.

ESCA has the advantage that the sensitivity factors are known. The data most closely related to our experiment are from angle-resolved ESCA at small electron emission angles. Based on a mean free path of $\lambda_e = 25$ Å one can easily calculate that ESCA taken at $\theta = 10°$ monitors a layer that has a thickness of $d \sim 4.3$ Å. For this situation Siegbahn *et al* [4] have measured the number of C atoms in TBAI compared with those in FA.

Taking into account the size of TBAI and FA as shown in table 2 we can state that the C atom of a surface FA molecule is clearly detected within the observation depth of $d = 4.3$ Å. However, it seems clear that only half of the TBA^+ ion lies within the observation depth. Thus, only half of the 16 C atoms of TBA^+ will be detectable. Accordingly, we have to divide the number of detected TBA^+ C atoms by eight in order to obtain the number of TBA^+ ions. This consideration is valid irrespective of the exact sampling depth d as long as it is smaller than the diameter of TBA^+ ions which is approximately 10 Å.

Table 2. Properties of relevant species [a]Siegbahn *et al* [4], [b]Kittel [24], [c]Morgner *et al* [1].

Species	Volume	Spherical shape		Cubic shape	
		Radius	Area	Length	Area
	Å^3	Å^2	Å^2	Å	Å^2
TBAI	500[a]	4.92	76.2	7.94	63.0
I^-	42.2	2.16[b]	14.7		
TBA^+	458	4.78	71.8		
FA	66.2[c]	2.51	19.8		

In this way we have obtained the number of TBA^+ ions normalized to the number of FA molecules in the surface. The values are also given in figure 8. They compare well with the ratio of I^- ions to FA molecules as given in the figure.

This result together with the finding from [3] that no differential effect between I^- ions and TBA^+ counter ions was found in ESCA seems to suggest that the number of I^- and TBA^+ ions in the outermost surface layer are identical. However, we have no unambiguous proof that the MIES sensitivities for I^- and FA are identical. It could still be that I^- ions are detected with a higher probability than FA molecules, as stated earlier, thus reducing the number of I^- within the topmost layer below the number of TBA^+ ions. The rest had then to be accommodated right below the topmost layer, still visible to ESCA but inaccessible to MIES. We will discuss this possibility later.

The second remarkable feature is the finding that I^- at the surface reacts with He^* as expected for a free ion. This is borne out by the value of the fine-structure splitting as well as by the relative population of the two fine-structure states $I(^2P_{1/2}, ^2P_{3/2})$. We have to conclude that I^- is exposed to a very isotropic environment. Model calculations show that anisotropic interactions must be smaller by at least an order of magnitude compared with the situation of I^- forming part of a butyliodide molecule [20].

If we are attempting to build up a model for the surface structure we are bound to avoid anisotropies around the I^- ions. Accordingly, the most natural idea that pairs of TBA^+ and I^- ions could form isolated units must clearly be discarded. This would result in a typical molecular value of the fine-structure splitting, see figure 7.

We have conceived two different models. In the first one, we let I^- be surrounded by a solvation shell of FA molecules. This keeps the cations TBA^+ at a sufficient distance that they cannot disturb the isotropy too much. The mere fact that I^- sits in the surface layer breaks spherical symmetry around the ion. This is, however, not an unambiguous reason to discard this possibility. For comparison, we note that Xe atoms adsorbed on a graphite surface are exposed to a similar break of spherical symmetry and still retain the atomic fine-structure splitting [21]. The degeneracy of

the sublevels of $Xe^+(^2P_{3/2})$ is lifted in that situation, but the observed splitting of 0.35 eV would be undetectable in our experiment due to the large FWHM of the peak (figure 5).

Our second model guarantees the isotropic environment of the I^- ions by surrounding it evenly by TBA^+ counter ions. Electrostatic stability requires that a structural unit essentially contains an equal number of anions and cations. Accordingly we have to conceive two-dimensional clusters of ions, large enough to make rim sites less probable than inner sites for the I^-. The questions of stability and electric field isotropy within such a cluster will be addressed later.

4.1. Model I of surface structure for $m \sim 0.9$ (solvation shell for I^-)

In the following we consider the structure of a surface as viewed by an incident He* atom. Thus, in the present context by solvation shell we mean a two-dimensional structure. The ionic radius of I^- is slightly smaller than the radius assigned to FA (see table 2). The two-dimensional shell around I^- is composed of six FA molecules.

This would lead to a ratio of I^- to FA of $\frac{1}{6} = 0.16$ in contrast to the values given in figure 7 for large concentrations. We have two possibilities:

(i) either we accept the equal detection probability for I^- and FA assumed in the evaluation of the data in figure 7. In consequence we have to abandon the isotropic solvation shell around every surface I^-; or

(ii) we assume that the detection probability of I^- is twice that of FA in MIES. Then we had to scale down the values in figure 7 by a factor of two and obtain agreement with the ratio of $I^-/FA \approx 0.16$ required by the solvation shell model. The consequence of this assumption would be that the number of surface I^- ions is only one half the number of TBA^+ ions in the surface. At the same time this would produce the proper ratio of 1/3 between TBA^+ ions and FA molecules. However, another problem arises then: it is not possible to find an arrangement of the solvated I^- and TBA^+ ions that prevents immediate contact between two or more cations. The strong Coulomb repulsion between neighbouring TBA^+ molecules (potential energy 2.7 eV) makes such a structure highly unlikely. In order to stabilize the situation one had to add FA molecules to the surface layer thus disturbing the balance between the numbers of TBA^+ ions and FA molecules again. Furthermore, this surface structure would invoke the existence of an electric double layer which is in contrast to our experimental findings, see the discussion later.

Based on these considerations we have concluded that model I does not yield a satisfying explanation for the experimental data.

4.2. Model II of surface structure for molality ~ 0.9 clusters of TBA^+ and I^- ions

In this model we conceive a two-dimensional cluster composed of TBA^+ and I^- ions. If every I^- ion is surrounded by, say, four cations the isotropy of the environment is well guaranteed. Model calculations with neutral two-dimensional clusters of point charges with NaCl structure gave the following picture:

(i) sizable potential gradients exist only at edge sites of a cluster (as expected);

(ii) upon variation of cluster shape and cluster size we find that increasing stability (i.e. binding energy/ion) correlates with decreasing absolute values of potential gradients; and

(iii) even in a small cluster—composed of eight ion pairs—the electric field strength is distinctly below the situation within an isolated ion pair. The maximum amounts to 50%, the averaged value to 15% of the ion-pair case. With increasing cluster size the potential gradients are reduced considerably.

The equal number of positive and negative ions in a cluster has a consequence on the assumed detection probability in MIES: it must be equal for both the I^- ions and FA molecules. From figure 7 we take the information that at molalities of approximately 0.9 we get one TBAI molecular unit per three FA molecules. This gives us a handle on the minimum cluster size. We have to conceive a shell of solvent molecules around every cluster. Two neighbouring clusters can either be separated by only one layer of FA molecules (shared shell) or both can have their own solvation shell (separated shell). The maximum number of TBAI molecules per FA molecule is given as a function of cluster size in figure 10. For the shared shell situation we need a cluster size of 11 to satisfy the experimental value of $N^{surf}_{TBAI}/N^{surf}_{FA} = 0.3$, in the separated shell case the clusters must contain 22 molecules or more.

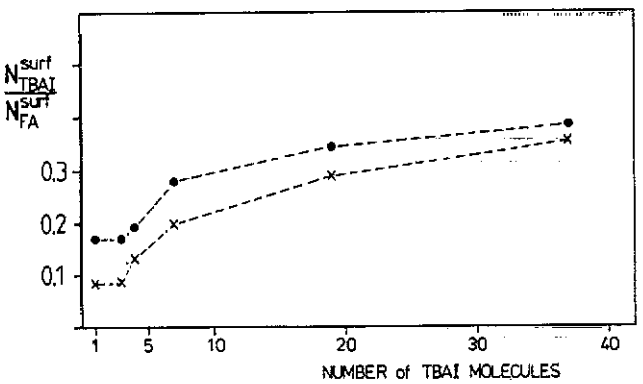

Figure 10. Two-dimensional NaCl-type cluster model of the surface of TBAI–FA solutions. The maximum number of TBAI molecules in the surface normalized to the number of FA molecules is given as function of cluster size (number of TBAI molecules per cluster). The results are based on the molecular areas in table 2. Dots, based on the assumption that adjacent clusters share the shells of solvent FA molecules; crosses, based on the assumption that adjacent clusters have separated shells of FA molecules. For further explanation see text.

These values are to be understood as lower bounds since the data in figure 10 are computed assuming that FA occurs in the surface only as part of solvation shells.

Another aspect of the cluster model gives a second handle on the cluster size. An I^- ion being part of a cluster will show an ionization energy that exceeds that of the isolated I^- by the amount of potential energy E_{pot} due to the other ions of the cluster:

$$IP[I^-/I^2P_{3/2}] = EA[I] - E_{pot}.$$

For all sites within a neutral cluster we find a negative value for the potential energy E_{pot} that varies with the site. This effect must show in the experiment in that it contributes to the peak width. If this were the only cause of peak broadening the corresponding full width of half maximum (FWHM) could be calculated from the variance σ of the E_{pot} values within a cluster:

$$\text{FWHM} = 2\sqrt{2 \cdot \ln 2} \cdot \sigma.$$

For the most stable cluster shapes we have calculated the FWHM normalized to the average of the potential energy as a function of cluster size. The results are shown in figure 11. In the upper panel we have added the electrostatic binding energy per ion normalized to the binding energy within an isolated ion pair. From the known electron affinity of iodine $EA = 3.069$ eV [22] and the observed binding energy in our experiment $IP = 6.75$ eV we can compute the relevant potential energy to be $E_{pot} = -3.7$ eV. The peak width in our experiment is 0.8 eV. The ratio $0.8/3.7 = 0.21$ has to be compared with the quantity $\text{FWHM}/\langle -E_{pot}\rangle$ in figure 11. We note that this criterion suggests a cluster size of $n \approx 21$, very close to the larger value found earlier. Again we have to point out that this value is a lower bound to the cluster size since other effects are also expected to cause peak broadening: for example band formation due to interaction between I^- ions and possible disorder within the cluster.

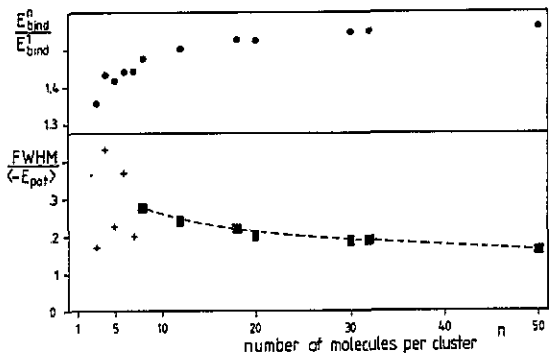

Figure 11. Two-dimensional NaCl-type cluster model of the surface of TBAI/FA solutions. Upper panel: stability of a two-dimensional cluster of point charges given as binding energy per ion normalized to binding energy in one ion pair. For all sizes the cluster shape with highest stability has been chosen. Lower panel: FWHM as computed from the variance of the energy values at all cluster sizes, normalized to the averaged potential energy. $\langle -E_{pot}\rangle$ can be identified with E_{bind} since in the frame of our point charge cluster electrons and negative ions are treated the same way.

If we assume an NaCl-type structure for the two-dimensional clusters as in our model calculations we can even attempt to determine the lattice constant from our data. We identify the additional binding energy of 3.7 eV mentioned earlier with the electrostatic potential energy calculated for our point charge cluster. If r is the distance between I^- and TBA^+ ions we find in our calculations:

$$E_{pot} = 1.55 \cdot V_{Coul}(r)$$

for cluster sizes $n \geq 20$. In the point charge model the factor can be identified with the normalized binding energy per ion E^n_{bind}/E^1_{bind} shown in figure 11. We see that this quantity depends only slightly on cluster size. From

$$V_{Coul}(r) = (1/1.55) \cdot (-3.7) \text{ eV}$$

we obtain $r = 6.03$ Å. In an NaCl structure this leads to a

$$\text{lattice constant } c = \sqrt{2} \cdot r = 8.53 \text{ Å}$$

and

$$\text{area of unit cell } a = c^2 = 72.7 \text{ Å}^2.$$

In view of the crudity of this approach this value agrees well with the area of the cross section of the TBAI molecule given in table 2.

In applying our point charge model to the TBAI clusters at the surface we have tacitly assumed that negative and positive ions lie in one and the same plane. If this were different, i.e. if the I^- ions form a plane separated by a distance h from the plane of the positive N^+ ions which represent the centre of charge in the TBAI groups we would have the effect of an electric double layer. The corresponding surface charge density at $m = 0.9$ is easily calculated: per TBAI molecule we have three FA molecules in the surface. If we sum the areas of these molecules we have the area per unit charge which results in the surface charge density

$$\sigma = 1/136 \text{ (e/Å}^2\text{)}.$$

The potential difference U is determined by the thickness of the double layer h to give

$$U = (\sigma/\varepsilon_0) \cdot h.$$

With the electric field constant $\varepsilon_0 = 5.53 \times 10^{-3} \text{e/(Å} \cdot \text{V)}$ we obtain

$$U = 1.33 \cdot h \text{ (V)}$$

if h is measured in Å.

A potential difference U due to double-layer formation should change the position of the vacuum level with respect to the Fermi energy. From the stability of the zero energy edge in our spectra upon adding TBAI to FA we infer that the vacuum level remains stable within ±100 meV. We have to conclude that the planes of positive and negative ions coincide within one-tenth of an Ångström.

It is interesting to view this result on the background of the crystal structure of related compounds. It is known that TBA trihalides [7] and tetramethyliodide [23] have structures that look more like a distorted CsCl than an NaCl crystal. Thus, if the clusters of TBAI that form at the surface of the solution resemble a cut through the crystal it may be conceived as a (110) plane rather than a (100) or (111) plane.

So far we have discussed the surface structure for molality 0.9, the highest concentration we have investigated. The abundance of I^- in the surface as function of molality (figure 8) suggests that the surface structure varies little with decreasing concentration down to $m \approx 0.25$. Below this concentration the ratio $N[I^-]/N[\text{FA}]$ drops to zero rather sharply. Even if one follows our earlier discussion about cluster formation at high concentrations one may speculate whether this feature carries through to $m \approx 0$. It seems conceivable that at low concentrations the ions appear in the surface with separate shells of FA molecules.

From the information in table 2 one can easily calculate the number of FA molecules needed to form a two-dimensional shell around the ions. This requires twelve FA molecules for TBA^+ and six for I^-. Thus, we find that the concept of ions with separate shells limits the ratio $N[I^-]/N[\text{FA}]$ to a maximum of 1/18=0.055. Our experimental data in figure 8 drop below this value at molality 0.07.

If one accepts these concepts—individual ions below molality 0.07 and stable clusters above ≈ 0.25—one has to consider the range in between as a situation in which the two principal structures compete. If we find a strong temperature dependence of the surface composition inside this range but not outside.

5. Summary

The surface of a solution of TBAI in FA has been discussed in the literature in terms of a concept of electrochemistry: the hydrophobic TBA^+ ions form an overlayer (first Helmholtz plane) and attract the I^- counter ions into a second layer. Due to the extreme surface sensitivity of MIES our data show unambiguously that I^- ions appear in the outermost surface layer. Furthermore we find that I^- behaves in the ionization process as if it is exposed to a very isotropic environment. This shows in the atomic-like fine-structure splitting and in the relative population of the fine-structure levels in MIES. From our data and making use of published ESCA results we have developed a model for the surface structure. The characteristic features are as follows: at high molal concentrations the surface is dominated by two-dimensional clusters of TBAI whereas at very low concentrations we have separate ions in the surface. In an intermediate range of concentrations the two structures compete which explains the strong temperature dependence of the surface composition.

Acknowledgments

We gratefully acknowledge financial support by the German Science Foundation (DFG) and by the Ministerium für Wissenschaft und Forschung des Landes Nordrhein-Westfalen.

References

[1] Morgner H, Oberbrodhage J, Richter K and Roth K 1991 *J. Electr. Spectr. Rel. Phen.* at press
[2] Ballard R E, Jones J and Sutherland E 1984 *Chem. Phys. Lett.* **112** 310
[3] Holmberg S, Moberg R, Zhong C Y and Siegbahn H 1986 *J. Electr. Spectr. Rel. Phen.* **41** 337
[4] Holmberg S, Zhong C Y, Moberg R and Siegbahn H 1988 *J. Electr. Spectr. Rel. Phen.* **47** 27
[5] Moberg R, Bökman F, Bohman O and Siegbahn H O G 1990 *Report 1219* Uppsala University Institute of Physics
[6] Adamson A W 1982 *Physical Chemistry of Surfaces* (New York: Wiley)
[7] Ferraro J R, Beno M A, Thorn R J, Wang H H, Webb K S and Williams J M 1986 *J. Phys. Chem. Solids* **47** 301
[8] Leisin O, Morgner H and Müller W 1982 *Z. Phys.* A **304** 23
[9] Keller W, Morgner H and Müller W A 1986 *Mol. Phys.* **57** 623; 1986 *Mol. Phys.* **58** 1039
[10] Kimura K, Katsumata S, Achiba Y, Yamazaki T and Iwata S 1981 *Handbook of HeI Photoelectron Spectra of Fundamental Organic Molecules* (Tokyo: Japan Scientific Societies Press)
[11] Moore Ch E 1949 *Atomic Energy Levels* NBS Series, Washington
[12] Hotop H 1971 *PhD Thesis* Freiburg
Hotop H and Niehaus A 1969 *Z. Phys.* **228** 68
[13] Hoffmann V and Morgner H 1979 *J. Phys.* B **12** 2857
[14] Wuilleumier F, Adam M Y, Dhez P, Sandner N, Schmidt V and Mehlhorn W 1977 *Phys. Rev.* A **16** 646
[15] Heckenkamp Ch, Schäfers F, Schönhense G and Heinzmann U 1986 *Z. Phys.* D **2** 257
[16] Haug B, Morgner H and Staemmler V 1985 *J. Phys.* B **18** 259
[17] Roth K 1990 *PhD Thesis* Witten, Germany
[18] Keller W, Morgner H and Müller W A 1986 *Mol. Phys.* **57** 637
[19] Müller W A 1986 *PhD Thesis* Freiburg
[20] Morgner H 1991 unpublished results
[21] Schönhense G, Eyers A and Heinzmann U 1986 *Phys. Rev. Lett.* **56** 512
[22] Hotop H and Lineberger W C 1975 *J. Phys. Chem. Ref. Data* **4** 539
[23] Herrschaft G and Hartl H 1989 *Acta Crystallogr.* C **45** 1021
[24] Kittel Ch 1983 *Einführung in die Festkörperphysik* (Munich: Oldenbourg)